Current Biology, Volume *20*

Supplemental Information

A Direct Role for Cohesin in Gene Regulation and Ecdysone Response in Drosophila Salivary Glands

Andrea Pauli, Joke G. van Bemmel, Raquel A. Oliveira, Takehiko Itoh, Katsuhiko Shirahige, Bas van Steensel, and Kim Nasmyth

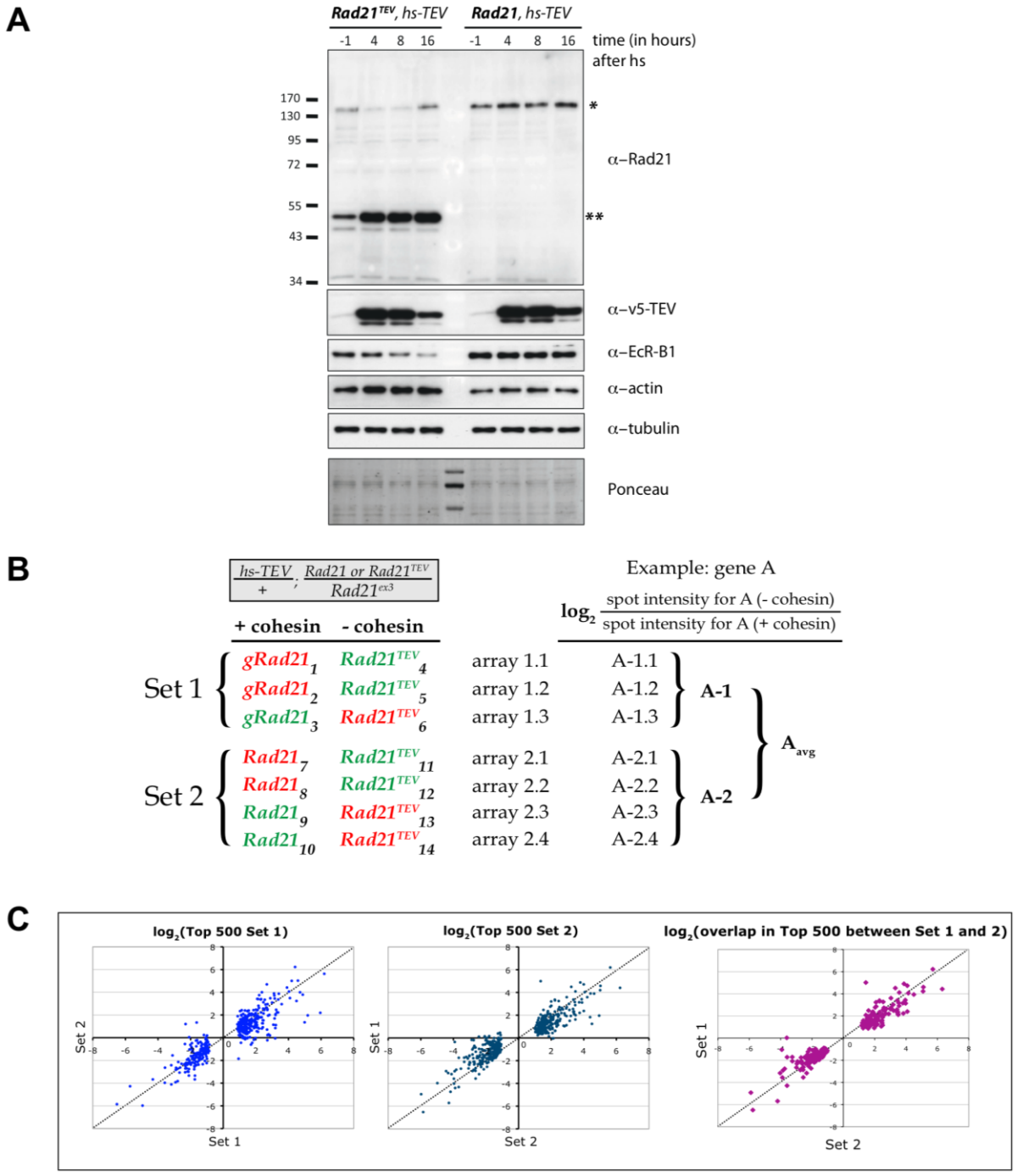

Figure S1. Differential Gene Expression Profiling by Microarrays after TEV Cleavage of Cohesin (Related to Figure 1)

(A) Cleavage of cohesin in salivary glands using the hs-TEV system. Western blot analysis of salivary gland extracts from *hs-TEV* crawling third instar larvae surviving either on Rad21^{TEV} or Rad21. Extracts were prepared before (t = -1; TEV off) and at different time points after a 45 minute heat shock at 37°C (the end of heat shock was set as t = 0). Blots were probed with the indicated antibodies. Full-length Rad21 (*) and the C-terminal TEV cleavage fragment (**) are marked. Tubulin and Ponceau stainings were used as loading controls.

(B) Overview of the seven individual microarray experiments and subsequent data analysis used for differential gene expression profiling of third instar larval salivary glands after heat shock-induced TEV cleavage of cohesin. Two sets of microarray experiments were performed, with three arrays in Set 1 (sample pairs *gRad21* and *Rad21TEV*) and four arrays in Set 2 (sample pairs *Rad21* and *Rad21TEV*). Cy3- (red) and Cy5 (green) labelled independent biological samples (numbered from 1 to 14) with (*gRad21* or *Rad21*) and without cohesin ($Rad21^{TEV}$) were hybridized in pairs to seven arrays. Spot intensities for each locus were measured for each channel separately and used to calculate $\log_2$-ratios (spot intensity in the presence versus absence of cohesin). Log_2-ratios were averaged across each set (e.g. values A-1 and A-2 for gene A) and across both sets (A_{avg}).
(C) Scatter plots comparing $\log_2$-ratios of the Top 500 genes of the two sets of experiments. Classification of genes as Top 500 was based on Limma statistical analysis. In the top two graphs, the $\log_2$-ratios of the Top 500 genes of Set 1 (light blue, left) were plotted against the corresponding $\log_2$-ratios of Set 2 and vice versa (dark blue, right). In the bottom graph (purple), $\log_2$-ratios of the 227 genes common between the Top 500 of Set 1 and Set 2 were plotted against each other. The diagonal indicates a hypothetical perfect correlation between both sets of data.

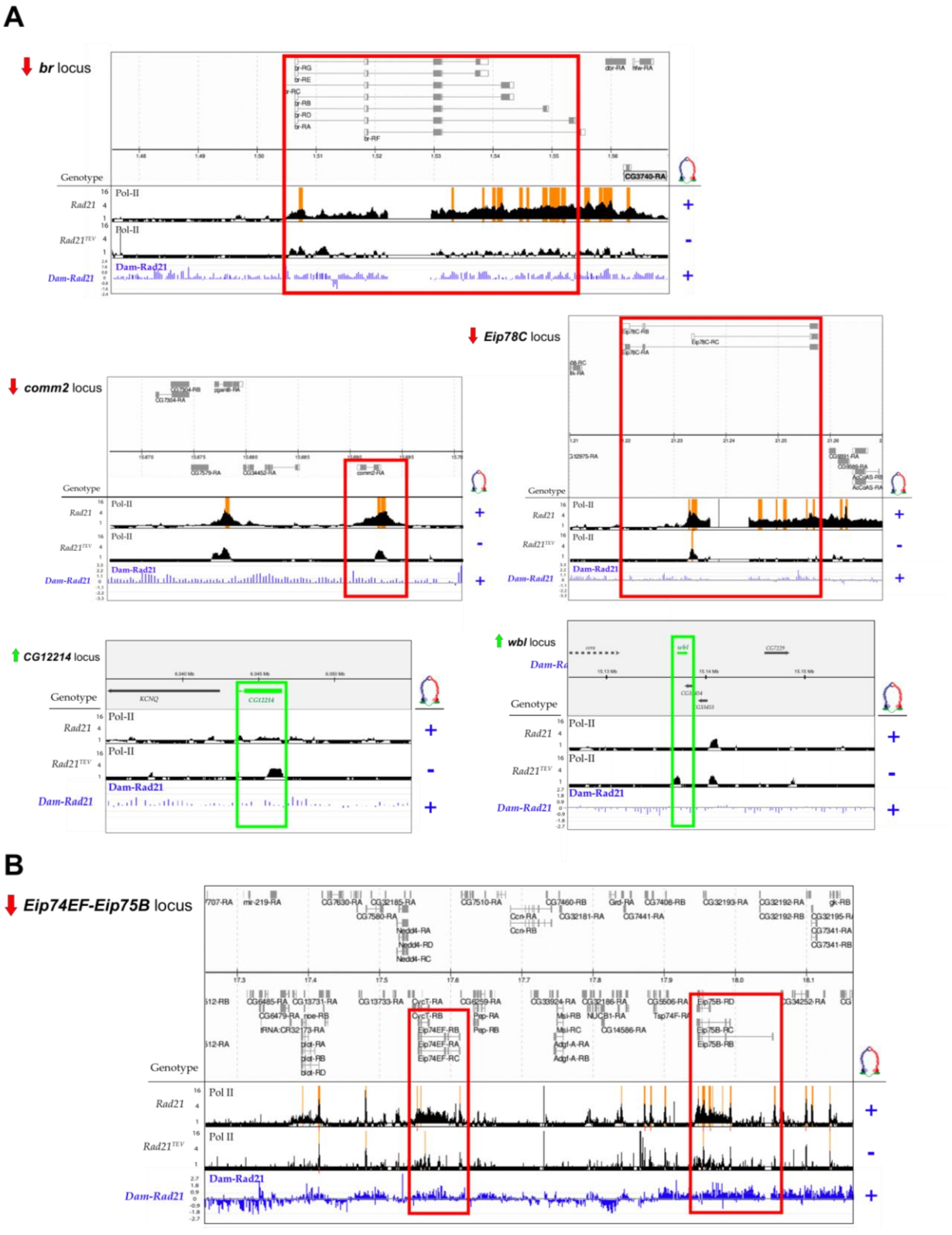
A
br locus
Genotype
Pol-II
Rad21
Rad21TEV
Dam-Rad21
Eip78C locus
comm2 locus
CG12214 locus
wbl locus
B
Eip74EF-Eip75B locus
Pol II

Figure S2. RNA Polymerase II (Pol-II) and Cohesin Binding Profiles at Differentially Expressed Loci (Related to Figure 1 and 2)

(A) Pol-II and cohesin binding at representative genomic loci whose expression changes in salivary glands upon cleavage of cohesin. ChIP-CHIP analysis was used to assess the distribution of Pol-II in *Rad21* (+ cohesin) and *Rad21TEV* (- cohesin) salivary glands 10-12 hours after heat shock induction of TEV protease (black plots). ChIP-CHIP data is represented as fold enrichment of IP over Input (MAT scores; log-scale; highly enriched regions ($p < 0.0001$) are coloured in orange). Cohesin binding in salivary glands was assessed by DamID (Dam-Rad21; blue plots) and is represented as the relative enrichment of methyladenine marked DNA from Dam-Rad21 glands over Dam-only glands (log2 scale).

(B) Pol-II and cohesin binding at the Ecdysone-regulated *Eip74EF* and *Eip75B* loci.

For further details see (A).

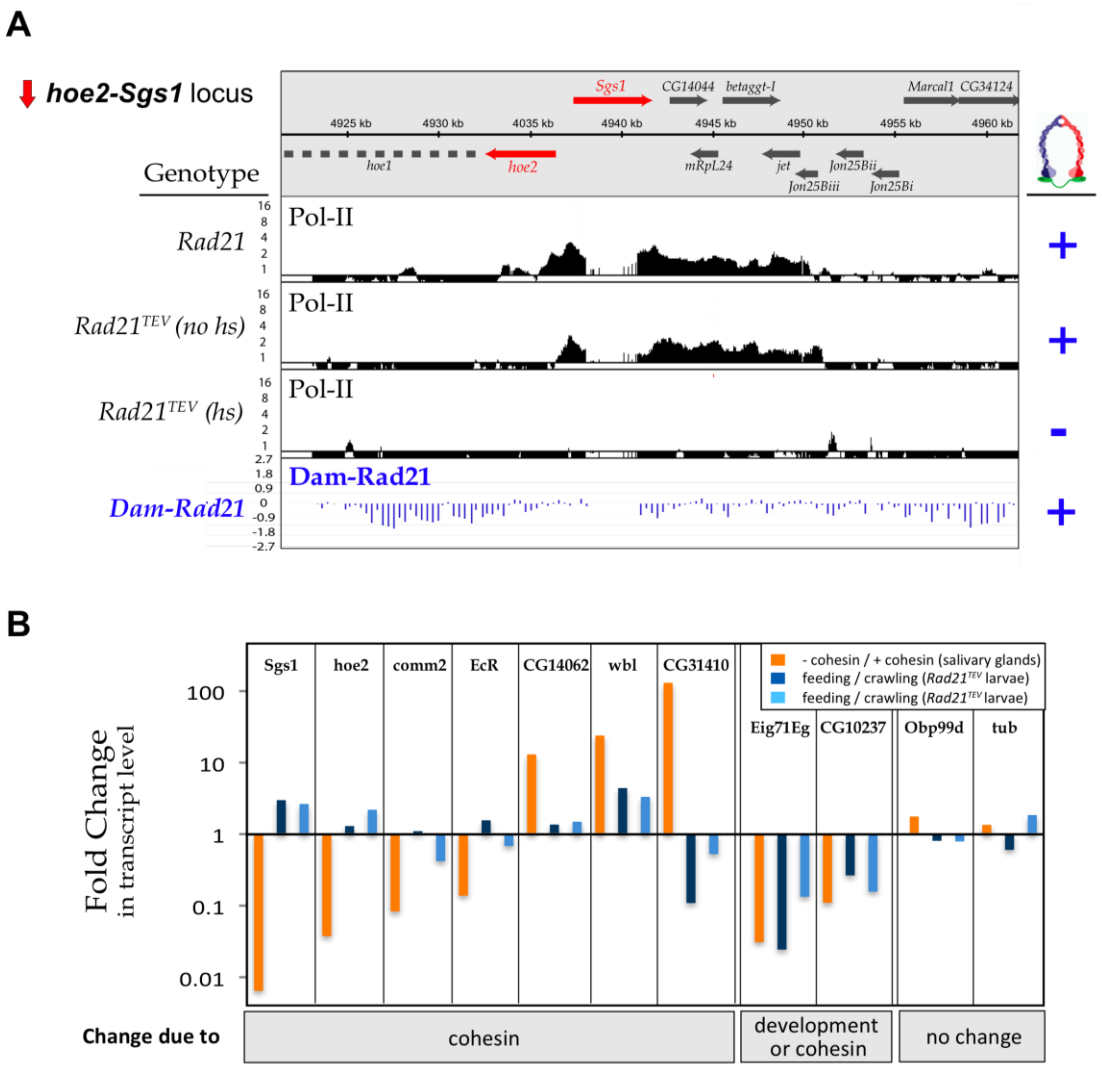

Figure S3. The Majority of Differences in Gene Expression Is Caused by Loss of Cohesin (Related to Figure 1 and 2)

(A) RNA Polymerase II (Pol-II) and cohesin binding profiles at the downregulated *Sgs1-hoe2* locus. Experimental details are as described in Figure legend S2, except that the Pol-II distribution is also shown for *Rad21*^{TEV} salivary glands carrying the uninduced *hs-TEV* transgene (no hs, + cohesin). Note that cohesin binds only at background levels to this locus (blue plot, DamID data).

(B) Comparison of gene expression differences observed after cohesin cleavage in salivary glands with those in younger versus older larvae. Transcript levels of 10 candidate genes (tubulin served as non-differentially expressed control) were measured by qRT-PCR. For each locus, the fold-change in transcript level in the absence versus presence of cohesin (orange bars) was compared to the fold-change in transcript level in feeding (younger) versus crawling (older) third instar *Rad21*^{TEV} (dark blue) or *Rad21* (light blue) larvae. Each value represents the average of at least two independent experiments.

Supplemental Tables
(See accompanying Excel spreadsheet)

Table S1. Genes Differentially Expressed in Salivary Glands upon Cohesin Cleavage (Related to Figure 1)
List of statistically significant (based on Limma statistical analysis), at least 1.5-fold upregulated genes (A, green) and at least 1.5-fold downregulated genes (B, red) upon cohesin cleavage in salivary glands, as identified by microarray analysis. Genes are sorted in descending order based on their average fold change in transcript levels in the absence versus presence of cohesin across seven independent microarrays. A minus indicates fold downregulation (see excel file).

Table S2. Gene Ontology (GO) Enrichment Analysis of Differentially Expressed Genes (Related to Figure 1)
Created in FlyMine (List Analysis tools) with the multiple hypothesis test correction of Benjamini and Hochberg ($p<0.01$) (see excel file)

Supplemental Experimental Procedures

Cloning of Dam-myc-Rad21

The coding region of untagged Rad21 was PCR-amplified using the primer pair Rad21_AP354_BglII_F (aaaAGATCTgATGTTCTATGAGCACATTATTTTGG) and Rad21_AP29_NotI_R (aaaGCGGCCGCATTAAAACAGATTTACATTCAAC) and a plasmid containing untagged Rad21 (pBS-Rad21 [1]) as template. The BglII/NotI-digested PCR product was cloned into the BglII/NotI-digested pCasper-hs-NDamMyc (Bas van Steensel, Henikoff lab) to generate a Dam-myc-Rad21 fusion construct. The Dam-myc-Rad21 insert was subcloned as EcoRI/XbaI fragment into a EcoRI/XbaI-cut pUAST vector.

DamID Analysis of Cohesin Binding in Salivary Glands

Genomic DNA was isolated from salivary glands of homozygous *Dam-Rad21* or *Dam-only* crawling third instar larvae by phenol-chloroform extraction. *In vivo* adenine-methylated fragments were amplified from genomic DNA by methylation-specific PCR as described before [2]. One microgram of amplified methylated DNA was labeled with Cy-dye labeled random nonamers (TriLInk Biotechnologies, according to NimbleChip Arrays User's Guide: ChIP-chip Analysis v2.0). Thirteen microgram of labeled Dam-Rad21 and 13 µg of Dam-only methylated fragments were pooled and hybridized to microarrays carrying 380,000 60-mer DNA oligonucleotides [3] (Roche-NimbleGen) with a median probe spacing of 300 bp. Material from two independent experiments was hybridized in opposite dye orientations. The obtained $\log_2$(Dam-Rad21/Dam-only) ratio reflects the extent of Rad21 binding to each probe, corrected for local differences in chromatin accessibility. Probes were mapped to *D.melanogaster* genome sequence Release 5.

Identification of Cohesin Domains

Rad21 domains were defined by using a two-state Hidden Markov Model. First, DamID log-ratios of biological replicates were averaged to give probe-wise scores. Because Dam methylates the sequence GATC, the smallest units of DamID mapping are GATC-flanked genomic fragments. Therefore, values from array probes mapping to the same GATC fragment were averaged to a single score. Target identification was carried out by fitting a Hidden Markov Model (HMM), which is a statistical framework that integrates scores of each probe and its neighboring probes to assign the most likely "bound" or "not bound" state. We used a modified version of an HMM algorithm that was previously described [4]. Details of this algorithm will be published elsewhere (Filion, van Bemmel and Braunschweig et al., manuscript submitted). An implementation of the algorithm in the R language (R Development Core Team, 2009) is available upon request.

Genes were classified as bound by cohesin based on the localization of their TSS (defined as the 1 kb region downstream of the transcriptional start) inside a Rad21 domain by using custom made R-scripts.

Pol-II Chromatin Immunoprecipitation (Chromatin IP)

Pol-II Chromatin Immunoprecipitations (Chromatin-IPs) of third instar larval salivary glands, using the CTD4H8 mouse anti-Pol-II antibody (Upstate), were performed according to [5] and [6] with minor modifications. For each Pol-II Chromatin IP, ~50 SG pairs were dissected in cold PBS and fixed in 1% (Pol-II ChIP) formaldehyde for 1.5 - 2 minutes at RT. Crosslinking was terminated by addition of 21.5 µl of 2.5 M Glycine (0.125 M final concentration) (3 minutes, RT, followed by 5 minutes on ice). Quenched samples were spun at 4000 rpm for 4 minutes, 4°C. The supernatant was discarded, and the crosslinked SGs were disintegrated in 100 µl of sonication buffer (0.5% SDS, 20 mM Tris pH 8, 2 mM EDTA, 0.5 mM EGTA, 0.5 mM PMSF, 1x complete protease inhibitors (Roche)) by pipetting. After 10 minutes on ice, samples were sonicated for 15 minutes in a Bioruptor, using the settings "high", 22 seconds ON, 60 seconds OFF, yielding chromatin fragments with an average size of 500 bp. Sonicated material was spun at 13000 rpm for 5 minutes, 4°C. 85 µl of the supernatant (100% IP) was used immediately for the IP, and 8.5 µl were stored at -20°C as 10% Input sample.

Each 85 µl ChIP-sample was diluted 10-fold in IP-Buffer (0.5% Triton X-100, 2 mM EDTA, 20 mM Tris pH 8, 150 mM NaCl, 10% glycerol, 1x complete protease inhibitors (Roche)) and precleared for 1-2 hours (4°C, rotating wheel) with 15 µl of Dynabeads® (Invitrogen) pre-equilibrated in IP-buffer. Beads were removed, and the supernatant was split in half and incubated with either 2.5 µl of mouse anti-Pol-II antibody (CTD4H8, Upstate) or 2.5 µl of normal mouse IgG (Millipore) (mock IP) (o.n., 4°C, rotating wheel). On the next day, 40 µl of pre-equilibrated Dynabeads® were added for 2-3 hours (4°C, rotating wheel) to capture the immuno-complexes. The supernatant was removed and the beads were washed in a series of 3-5 minute washes with cold buffers (1x Low Salt Buffer: 20 mM Tris pH 8, 2 mM ETDA, 0.1% SDS, 1% Triton X-100, 150 mM NaCl; 3x High Salt Buffer: same as Low Salt Buffer but 500 mM NaCl; 1x LiCl Buffer: 2 mM EDTA, 10 mM Tris pH 8, 0.25 M LiCl, 1% NP40, 1% Sodium-deoxycholate; 2x rinse with TE). Immuno-complexes were eluted and crosslinks were simultaneously reversed in 415 µl of Elution Buffer (100 mM Sodium-hydrogen-carbonate, 1% SDS, 0.181 M NaCl) for at least 6 hours (or o.n.) at 65°C under vigorous shaking. Crosslinks in Input samples were reversed in parallel after addition of 207.5 µl of Elution Buffer. Protein and RNA were digested with 14.9 µl (7.5 µl for Input samples) of an enzyme-mix containing 12 µl 1 M Tris pH 8, 1.6 µl Proteinase K (10 mg/ml) and 1.3 µl DNAse-free RNAse (10 mg/ml) (2 hours, 45°C). DNA was column-purified (Qiagen PCR-purification kit), eluted in 100 µl water and stored at -20°C.

To confirm efficient Chromatin-IP, an aliquot of each purified ChIP sample was used as template in a qRT-PCR reaction with a pair of "test-primers" before DNA was amplified for hybridization. For Pol-II ChIP samples, published primer combinations at the *hsp70* locus served as positive (amplicon +58) and negative control (amplicon +4080), amplifying the Pol-II enriched 5'end of the *hsp70* gene and the Pol-II depleted region 1600 bp downstream of the *hsp70* gene, respectively [7]. 5 µl of serially diluted Input samples (1:5 dilutions - 10%, 2%, 0.4%, 0.08%, 0.016%) and ChIP samples (1:2 dilutions - 100 %, 50 %, 25 %, 12.5 %) served as templates for qRT-PCR reactions. Cycle parameters for quantitative real-time PCRs for Pol-II ChIP samples were 15 min 95°C, 45 cycles of 10 seconds 95°C, 20 seconds 54°C, 40 seconds 72°C.

Linear Amplification of DNA by *In Vitro* Transcription

ChIP-enriched samples of ~50 salivary gland pairs were pooled, and DNA was linearly amplified by IVT (*in vitro* transcription) as described in [8]. Non-enriched 10% Input samples were processed in parallel. Briefly, ChIP DNA was de-phosphorylated by Calf Intestinal Alkaline Phosphatase (CIP, NEB) (0.25 µl of 10U/µl in a total volume of 10 µl) (1 hour, 37°C). DNA was purified with the MinElute Reaction Cleanup Kit (Qiagen) and eluted in 13.5 µl of DNAse-free water. CIP-treated DNA was poly-dT tailed (12.7 µl of dephosphorylated DNA, 4 µl 5x TdT reaction buffer (Roche), 0.6 µl 25 mM $CoCl_2$ (Roche), 0.92 µl 100 µM dTTP (TAKARA), 0.8 µl 10 µM ddCTP (TAKARA), 1 µl 400 U/µl Terminal Tranferase (Roche)) (20 minutes, 37°C). The reaction was stopped by addition of 4 µl of 0.5 M EDTA and DNA was cleaned-up with the MinElute Reaction Cleanup Kit (Qiagen). 12.3 µl of poly-dT-tailed DNA served as template for second strand synthesis and incorporation of the T7-promoter sequence (0.12 µl of 25 µM T7-polyA primer (for the sequence see Appendix VI.1), 4 µl 5x 2nd strand buffer, 1.6 µl 2.5 mM dNTPs) (2 minutes 94°C, 2 minutes 35°C, hold at 25°C). After addition of 2 µl of 2 U/µl DNA Polymerase (Invitrogen), the reaction was incubated for 90 minutes at 37°C. The reaction was stopped by addition of 5 µl of 0.5 M EDTA and DNA was cleaned-up with the MinElute Reaction Cleanup Kit (Qiagen). 10 µl of the purified DNA (in RNase-free water) served as template for the first round of IVT amplification by T7 RNA polymerase (4x 2.5 µl dNTPs, 10x Reaction Buffer, 2.5 µl enzyme mix (all MEGAscript T7 Kit, Ambion), 1.2 µl 200 U/µl T7 RNA polymerase (Ambion)) (16 hours , 37°C). RNA was purified with the RNeasy Mini Kit (Qiagen) and eluted in 40 µl of RNase-free water. The cRNA yield and amplification efficiency were determined by Nanodrop and BioAnalyzer (Agilent Technology). Due to insufficient material after the first round of IVT (< 10 µg), a second round of IVT amplification was performed after conversion of the cRNA into cDNA (random-primed first-strand SuperScript II Reverse Transcriptase-catalyzed cDNA synthesis (Invitrogen), T7-polyA-primed second-strand synthesis). cDNA was cleaned-up with the MinElute Reaction Cleanup Kit (Qiagen). 8 µl of the purified cDNA (in RNase-free water) served as template for the second round of IVT amplification by T7 RNA polymerase (see 1st round of IVT, except for 20 µl total volume and no additional T7 RNA polymerase). cRNA was purified with the RNeasy Mini Kit (Qiagen) and eluted in 40 µl of RNase-free water and checked for amplification efficiency by BioAnalyzer (Agilent Technology). 11 µg of cRNA served as template for double-stranded cDNA synthesis acording to manufacturer instructions (random-primed first-strand SuperScript II Reverse Transcriptase-catalyzed cDNA synthesis (Invitrogen) (2 hours, 42°C), followed by second-strand synthesis (Invitrogen) (2 hours, 16°C). RNA was removed by incubation with 3 µl of RNase cocktail (20 minutes, 37°C). cDNA was phenol-chloroform purified and dissolved in 22 µl of DNAse-free water. The cDNA yield (typically about 10 µg) was determined by measuring the absorbance at 260 nm (Nanodrop).

DNA Fragmentation and Labeling

10 µg of cDNA was fragmented with DNase I (up to 21 µl DNase-free water, 2.4 µl 10x One-Phor-All Buffer, 1.35 µl 25 mM $CoCl_2$ (Roche), 2.2 µl of 0.02 U/µl pre-diluted DNase I (Invitrogen)) (35 minutes, 37°C, followed by 15 minutes, 95°C). The fragment size of the cDNA (50-100 bp) was checked on a 2% Agarose gel. Fragmented cDNA was end-labeled with biotin (24.7 µl fragmented cDNA, 7.72 µl 5x TdT buffer (Roche), 3.86 µl 25 mM $CoCl_2$ (Roche), 2.5

mM biotin-N6-ddATP (NEL508, Perkin Elmer), 1.25 µl 40 U/µl Terminal Transferase (Roche)) (2 hours, 37°C, followed by 10 minutes, 95°C). Labeled samples were stored at -20°C until hybridization.

Hybridization to Affymetrix Whole Genome Arrays

A hybridization cocktail was prepared for each sample (ChIP-enriched sample or non-enriched Input control). 40 µl of fragmented and labeled DNA was mixed with 4 µl 3 nM control oligonucleotide B2 (Affymetrix), 2.4 µl 10 mg/ml Herring Sperm DNA, 2.4 µl 50 mg/ml acetylated BSA, 120 µl 2x Hybridization Buffer, 16.8 µl DMSO and 54.4 µl water. The hybridization cocktail was heated for 10 minutes to 100°C, followed by 5 minutes at 45°C and spun for 5 minutes at 15000 rpm to remove any insoluble material. All further procedures were preformed according to Affymetrix GeneChip instructions. Hybridization to Affymetrix GeneChip® *Drosophila* Tiling 2.0R arrays (containing 25-mer oligonucleotide probes interrogating the entire *Drosophila* genome, including repetitive sequences, with an average 38-base-pair spacing) was performed for 16 hours at 45°C, 60 rpm (Hybridization Oven 640, Affymetrix). After hybridization, arrays were washed in a Fluidics Station 450 (Affymetrix) and scanned with a GeneChip® Scanner 3000 7G (Affymetrix) with GeneChip® Operating Software (GCOS, Affymetrix).

Western Blot Analysis

Western Blot analysis was performed from dissected third instar larval salivary glands and whole larvae according to standard protocols. The following antibodies were used: guinea-pig α-Rad21 (1:3000 [1]), mouse α-v5 (1:5000; Invitrogen), mouse α-tubulin (DM1A) (1:8000; Sigma-Aldrich), mouse α-EcR-B1 (AD4.4) (1: 50; DSHB), rabbit α-actin (1:1000; Abcam ab1801), mouse α-Pol-II CTD4H8 (1:5000; Upstate), rat α-Rpb3 (1:500; [6]), rabbit α-pan-H3 (1:1000) and rabbit α-pan-H4 (1:1000, Upstate 05-858). HRP-linked secondary antibodies (Amersham) were detected by Enhanced Chemi-Luminescence (ECL) (Amersham).

qRT-PCR with cDNA Samples

cDNA for quantitative real-time PCR was synthesized from Trizol-isolated total RNA according to manufacturer instructions, using oligo-(dT)-primer and Superscript® II Reverse Transcriptase (Invitrogen). A fixed amount of *in vitro* transcribed exogenous mRNA (EGFP-tagged human *Bub1* mRNA, kindly provided by Barry McGuinness) was included in each cDNA synthesis reaction and served as internal reference for normalization of qRT-PCR reactions. To confirm the absence of contaminating genomic DNA in total RNA preparations, each cDNA synthesis reaction was also performed without Reverse Transcriptase (-RT, negative control). qRT-PCRs reactions (performed in duplicates) were setup by the automated CAS-1200™ instrument (CAS Robotics 4 (Version 4.9.1), Corbett Research), and run on the Rotor-Gene RG-3000 Thermocycler (Corbett Research). Primers used to test for differential expression in the absence/presence of cohesin are listed in Supplemental Experimental Procedures. The threshold cycle (Ct) values were calculated automatically by the Rotor-Gene Analysis Software 6.1 (Build 81, Corbett Research). All further analysis and calculations were performed in Microsoft Excel.

Ct-values for cDNA preparations with Reverse Transcriptase were typcially 10 to 15 Ct-values lower than those obtained for templates prepared in the absence of Reverse Transcriptase (-RT).

Normalized Ct (ΔCt)-values for each sample were calculated by subtracting the Ct-value obtained for each endogenous transcript from the Ct-value for the corresponding exogenous GFP transcript ($\Delta Ct = Ct_{GFP} - Ct_{endogenous\ tx}$). The GFP-normalized values for each transcript were calculated with the formula $2^{\Delta Ct}$. The relative fold-enrichment of a specific transcript in the absence versus presence of cohesin (-/+ cohesin) was determined by dividing the GFP-normalized value of transcript X in the absence of cohesin by the GFP-normalized value of transcript X in the presence of cohesin ($\text{fold-enrichment}_{-/+\ cohesin} = 2^{\Delta Ct}{}_{-cohesin} / 2^{\Delta Ct}{}_{+cohesin}$).

Oligonucleotides for Quantitative RT-PCR

Sgs1_AP406_F	CCGATACTCCACCATGCACCTGTTCT
Sgs1_AP407_R	GGGTTGTTTGGGTTCCTTGGGTTG
Hoe2_AP396_F	CCTTGGAACGCTTGGATTTGTGATG
Hoe2_AP397_R	GAGGATGAGGATGGATACGAGGAGGTG
Comm2_AP416_F	TCCTGGCTGCTCCTCTCCTGCTT
Comm2_AP417_R	GCTCCTGCTTCCTGTACCATCAGTTCC
EcR-B1_AP448_F	CTCATCAACTCCACAACGCCCTCAAC
EcR-B1_AP449_R	CGCCTCCGCCTACTCCAAGACCTAC
Cue_AP468_F	GCATTGTGCGGAAGGTGAAGGA
Cue_AP469_R	TCAACAGACGACAGAAAAGGGAGCA
CG9040_AP452_F	TAGACGGCGCAGGCGCACCAC
CG9040_AP453_R	CTGGACTCTACATCAGAGTCGTCA
CG12214_AP456_F	TCGGTGGTTAGTTGAGCGTTTGGTG
CG12214_AP457_R	GGTCTGGGCTGGTTTTTGGAGTGTATTTT
CG9737_AP466_F	AAAAGAGCCAACAGACGCAGGACAAAA
CG9737_AP467_R	TCCACATTCCGCACTCATTCACTCAC
Ush_AP464_F	ATACCGCAGAAGAGATGACCGTCG
Ush_AP465_ush_R	TTTTCTGGCTCCTCGAACTCAGCA
Wbl_AP434_F	GGTGTCAAGGACTATGGAGAACTGGAGA
Wbl_AP435_R	CCCTTGAACAGGAAGATACTCGGGAAG
CG31410_AP430_F	GGCCACCACAACGGCAAAGG
CG31410_AP431_R	CGGGAACGAAGGCTCCACATAGAAG
Mst87F_AP360_F	GGTTCTATCCTATCGTCTTGGTGTTCTGGTG
Mst87F_AP361_R	TGCGGACCCTGTGGACCCTGCTGC
Eip74EF_AP534_F	GCCACCGCTCTGCTCCACATAAA
Eip74EF_AP535_R	CGGGACTGGGCGGAAATGAAC
Eip75B_AP536_F	GCCATGCAACAGAGCACCCAGA
Eip75B_AP537_R	AAACATGCAGATCAGGCGCACAAAC
CG31698_AP370_F	TCTGCTTGCCCCACGAAAATGAAA
CG31698_AP371_R	CCACCTCGGGATAACGCCTGCT
RplII215_AP544_F	CGGACTCGAAGGCGCCGTTG
RplII215_AP545_R	TGTCTTGGTGATGAAGCCGATGTGGA
Act5c_AP540_F	GACACCAAACCGAAAGACTT
Act5C_AP541_R	ACCCACGTACGAGTCCTTCT
Tub_2075_F	GGCGGAACGCAATGACA
Tub_2152_R	CGCCACACCAACGATAACG

Fly Strains

Genotype	Abbreviation	Source
w^{1118}	*w*	Bloomington
w; P[w+, tubpr-Gal80^{ts}] (III)	*tubGal80^{ts}*	[9]
Gal4 driver		
w; P[w+, GawB]F4 (II)*	*F4-Gal4*	[10]
Rad21-excisions (*Rad21^{ex}*)		
w; Rad21 ^{ex3}/TM3, Sb, Kr-Gal4, UAST-GFP	*Rad21 ^{ex3}*	[1]
y, w; Rad21 ^{ex15}/TM3, Sb, Kr-Gal4, UAST-GFP	*Rad21 ^{ex15}*	[1]
Rescued *Rad21^{ex}* strains		
w; Rad21^{ex15}, P[w^{+}, tubpr<Rad21(550-3TEV)-myc$_{10}$<SV40] (III)	*Rad21^{TEV}*	[1]
w; Rad21^{ex3}, P[w^{+}, tubpr-Rad21-myc$_{10}$-SV40] (III)	*Rad21*	[1]
w; Rad21^{ex15}, P[w^{+}, tubpr<Rad21(550-3TEV)-myc$_{10}$<SV40], polyUbi-His2A-mRFP1 (III)	*His2Av-mRFP, Rad21^{TEV}*	[11]
TEV-protease strains in Rad21-mutant background		
w; P[w+, hs-NLS-v5-TEV-NLS2]; Rad21 ^{ex3}/TM6B, Tb, ubiquitin-GFP	*hs-TEV ; Rad21^{ex3}/TM6B, Tb*	[1]
w; Rad21 ^{ex15}, P[w+, UAS-NLS-v5-TEV-NLS2]/TM3, Sb, Kr-Gal4, UAST-GFP	*Rad21 ^{ex15}, UAS-TEV/TM3, Sb, Kr>GFP*	[1]
w; Rad21 ^{ex15}, P[w+, tubpr-Gal80^{ts}], P[w+, UAST-NLS-v5-TEV-NLS2]/ TM6B, Tb, ubiquitin-GFP	*Rad21 ^{ex15}, tubGal80^{ts}, UAS-TEV/ TM6B, Tb*	Present study
w; Rad21 ^{ex15}, P[w+, tubpr-Gal80^{ts}], P[w+, UAST-NLS-v5-TEV-NLS2]/ TM6B, Tb, ubiquitin-GFP	*Rad21 ^{ex15}, tubGal80^{ts}, UAS-TEV/ TM6B, Tb*	Present study
w; P[w+, GawB]F4; Rad21 ^{ex15}, P[w+, tubpr-Gal80^{ts}], P[w+, UAST-NLS-v5-TEV-NLS2]/TM6B, Tb, ubiquitin-GFP	*F4-Gal4; Rad21 ^{ex15}, tubGal80^{ts}, UAS-TEV/ TM6B, Tb*	Present study
Fly stocks for DamID		
w; P[w+, UAST-Dam-myc-Rad21] (X)	*Dam-Rad21*	Present study
w; P[UAST-Dam, w[+mC]] 1-1M/ TM6B	*Dam-only*	[12]

Supplemental References

1. Pauli, A., Althoff, F., Oliveira, R.A., Heidmann, S., Schuldiner, O., Lehner, C.F., Dickson, B.J., and Nasmyth, K. (2008). Cell-type-specific TEV protease cleavage reveals cohesin functions in Drosophila neurons. Developmental Cell *14*, 239-251.
2. Greil, F., Moorman, C., and van Steensel, B. (2006). DamID: mapping of in vivo protein-genome interactions using tethered DNA adenine methyltransferase. Methods Enzymol *410*, 342-359.
3. Choksi, S.P., Southall, T.D., Bossing, T., Edoff, K., de Wit, E., Fischer, B.E., van Steensel, B., Micklem, G., and Brand, A.H. (2006). Prospero acts as a binary switch between self-renewal and differentiation in Drosophila neural stem cells. Dev Cell *11*, 775-789.
4. Humburg, P., Bulger, D., and Stone, G. (2008). Parameter estimation for robust HMM analysis of ChIP-chip data. BMC Bioinformatics *9*, 343.
5. Adelman, K., Marr, M.T., Werner, J., Saunders, A., Ni, Z., Andrulis, E.D., and Lis, J.T. (2005). Efficient release from promoter-proximal stall sites requires transcript cleavage factor TFIIS. Mol Cell *17*, 103-112.
6. Yao, J., Ardehali, M.B., Fecko, C.J., Webb, W.W., and Lis, J.T. (2007). Intranuclear distribution and local dynamics of RNA polymerase II during transcription activation. Mol Cell *28*, 978-990.
7. Ni, Z., Schwartz, B.E., Werner, J., Suarez, J.R., and Lis, J.T. (2004). Coordination of transcription, RNA processing, and surveillance by P-TEFb kinase on heat shock genes. Mol Cell *13*, 55-65.
8. Wendt, K.S., Yoshida, K., Itoh, T., Bando, M., Koch, B., Schirghuber, E., Tsutsumi, S., Nagae, G., Ishihara, K., Mishiro, T., et al. (2008). Cohesin mediates transcriptional insulation by CCCTC-binding factor. Nature *451*, 796-801.
9. Buttitta, L.A., Katzaroff, A.J., Perez, C.L., de la Cruz, A., and Edgar, B.A. (2007). A double-assurance mechanism controls cell cycle exit upon terminal differentiation in Drosophila. Dev Cell *12*, 631-643.
10. Weiss, A., Herzig, A., Jacobs, H., and Lehner, C.F. (1998). Continuous Cyclin E expression inhibits progression through endoreduplication cycles in Drosophila. Curr Biol *8*, 239-242.
11. Oliveira, R.A., Hamilton, R.S., Pauli, A., Davis, I., and Nasmyth, K. (2010). Cohesin cleavage and Cdk inhibition trigger formation of daughter nuclei. Nat Cell Biol *12*, 185-192.
12. Vogel, M.J., Pagie, L., Talhout, W., Nieuwland, M., Kerkhoven, R.M., and van Steensel, B. (2009). High-resolution mapping of heterochromatin redistribution in a Drosophila position-effect variegation model. Epigenetics Chromatin *2*, 1.